Evaluating stiffness and strength of pavement materials

Article *in* Geotechnical Engineering · January 2005

DOI: 10.1680/geng.2005.158.4.217

CITATIONS
21

READS
2,663

2 authors:

Tuncer B. Edil
University of Wisconsin–Madison
366 PUBLICATIONS **8,479** CITATIONS
SEE PROFILE

Auckpath Sawangsuriya
Government Organization
32 PUBLICATIONS **397** CITATIONS
SEE PROFILE

Proceedings of the Institution of Civil Engineers
Geotechnical Engineering 158
October 2005 Issue GE4
Pages 217–230

Paper 13910

Received 19/07/2004
Accepted 12/01/2005

Keywords:
pavement design/quality control/ strength & testing of materials

Auckpath Sawangsuriya
Graduate Research Assistant, Department of Civil and Environmental Engineering, University of Wisconsin-Madison, USA

Tuncer B. Edil
Professor, Department of Civil and Environmental Engineering, University of Wisconsin-Madison, USA

ice

Evaluating stiffness and strength of pavement materials

A. Sawangsuriya MSc and T. B. Edil PhD, PE

Current mechanical empirical-based pavement design requires use of the mechanical properties of pavement materials. For quantitative evaluations of the mechanical properties (i.e. stiffness and strength), field tests are emphasised. In this paper, a recently developed instrument called the soil stiffness gauge (SSG) and the dynamic cone penetrometer (DCP) have been used to assess respectively the in-situ stiffness and strength of natural earthen materials, industrial by-products, and chemically stabilised soils from ten highway construction sites around the state of Wisconsin, USA. The SSG and DCP survey data were analysed to develop a relationship between the SSG stiffness and DCP penetration index (DPI) values for individual material types and for all materials combined. A simple linear semi-logarithmic model is obtained between the SSG stiffness and DPI values, with the coefficient of determination, R^2, ranging from 0·47 to 0·75 for individual material types and an R^2 value of 0·72 for all materials combined. The SSG stiffness and DPI values can be also correlated with the modulus (E) and California bearing ratio (CBR) of the materials respectively. A good relationship is obtained between E from the SSG and CBR from the DCP, and is compared with the well-known equations developed by Powell *et al.* and AASHTO as well as other available correlations from different in-situ tests: the falling weight deflectometer, German light drop weight, and plate load tests. Finally, the proposed power model is validated with a data set from two other test sites. Either or both devices show good potential for future use in pavement and subgrade materials evaluation. The in-situ stiffness and strength properties of various materials can be rapidly and directly monitored in companion with the conventional compaction control tests during pavement construction. The modulus of pavement and subgrade materials is uniquely related to CBRs regardless of soil type and site, and their relationship is also applicable to both as-compacted and post-construction states.

NOTATION

CBR	California bearing ratio
C_u	coefficient of uniformity
D_{10}	particle diameter corresponding to 10% finer
D_{60}	particle diameter corresponding to 60% finer
DPI	dynamic cone penetrometer (DCP) penetration index
DPI_{avg}	arithmetic average of DPI value
$DPI_{wt\ avg}$	weighted average of DPI value
E	modulus
E_{DCP}	modulus from the DCP test
E_{FWD}	back-calculated modulus from the FWD test
E_{LDW}	modulus from the light drop weight test
E_{PLT}	modulus from the plate load test
E_{RM}	modulus from the resilient modulus test
E_{SEIS}	modulus from the seismic test
$E_{SEIS\text{-}MOD}$	modulus from the seismic test after adjustment to realistic stress and strain levels for the pavement
E_{SSG}	modulus from the SSG test
K_{SSG}	SSG stiffness
LL	liquid limit
PI	plasticity index
R^2	coefficient of determination
$S_{u1\cdot0\%}$	stress causing 1% axial strain
W_N	natural water content
W_{OPT}	optimum water content
γ_{dmax}	maximum dry unit weight
ν	Poisson's ratio of the materials
$\sigma_1-\sigma_3$	deviator stress
σ_3	confining stress

1. INTRODUCTION

Given the importance of the mechanical properties (i.e. stiffness and strength) in pavement materials evaluation, there has been a concerted effort in recent years to develop methods for quantitative evaluations of these properties. Direct monitoring of stiffness and strength is consistent with the transition from empirical to current mechanistic-empirical pavement design procedures for structural design of flexible pavements. To successfully implement mechanistic-empirical pavement design procedures, and to move toward the performance-based specifications that are required to control the long-term functional and structural performance, additional in-situ stiffness and strength measurements should be included along with the conventional compaction control tests (i.e. nuclear density or laboratory moisture content samples), which do not give the mechanical properties of pavement materials directly.[1,2] Direct monitoring of stiffness and strength would facilitate quantitative evaluations of alternative construction practices and materials, such as recycled and reclaimed materials, that result in cost savings and environmental benefits.[2] For instance, the use of recycled and reclaimed

materials, both as working platform over poor subgrade and as a subbase in pavement structure, is being explored by the transportation community. Evaluation of these new materials on the basis of index property measurements such as moisture density or past subjective experience based on natural soil behaviour is also severely limited. Most of the correlations for modulus (E) are based on water content, dry density, and degree of saturation, and were developed from tests on laboratory-compacted specimens. Because field compaction curves and the associated lines of optimum are often different from those of laboratory compaction, and also the moisture condition of pavement materials changes with time after construction, the use of these laboratory-based correlations may cause significant error in estimating the operating pavement and subgrade moduli. Empirical correlations based on California bearing ratio (CBR)[3,4] or stress causing 1% strain ($S_{u1{\cdot}0\%}$) in the unconfined compression test[5] have been successfully used in evaluating pavement and subgrade moduli. Moreover, the relationship between E and CBR or E and $S_{u1{\cdot}0\%}$ is not affected by the changes in subgrade condition after construction and therefore is applicable to both as-compacted and post-construction states.

The soil stiffness gauge (SSG), a recently developed instrument, and the dynamic cone penetrometer (DCP), which is commonly used by the pavement community, offer a means of directly monitoring the in-situ stiffness and index of strength of surficial materials. SSG stiffness and DCP penetrometer index (DPI) have been also correlated with modulus and CBR respectively.[6,7] In this study, these two devices will be implemented in a number of projects over two construction seasons in the state of Wisconsin, USA. The objectives of this study are:

(*a*) to examine the use of the SSG and DCP for pavement materials evaluation
(*b*) to explore the degree of correlation and appropriate effective depth zone for statistically significant empirical correlations between the two devices
(*c*) to develop the modulus and CBR relationship obtained from these devices and compare it with the other well-known relationships as well as with different in-situ tests.

2. SOIL STIFFNESS GAUGE (SSG)

2.1. Description

The soil stiffness gauge (SSG), which is currently marketed as the Humboldt GeoGauge™ (Fig. 1(a)), is a recently developed instrument for directly measuring the in-situ stiffness of soils. The SSG measures near-surface stiffness by imparting a small dynamic force to the soil though a ring-shaped foot at 25 steady-state frequencies between 100 and 196 Hz. Based upon the force and displacement–time history, the stiffness is calculated internally as the average force per unit displacement over the measured frequencies and reported. In a previous investigation, the acceleration and corresponding displacement were measured.[6] Given knowledge of the soil properties, the force induced by the SSG was estimated based on finite element analysis. The maximum single amplitude dynamic force produced during the SSG measurement is determined to be 10 to 17 N. A measurement takes only about 1·5 min. Sawangsuriya *et al.*[8] studied the zone of measurement influence and the effects of layered materials on the SSG measurement in granular materials. A finite element analysis and the SSG measurements in a test box indicated that the radius of measurement influence extends to 300 mm. For two-layer materials with different stiffness, the SSG starts to register the stiffness of an upper-layer material of 125 mm or thicker. The effect of the lower layer may continue to be present even at an upper-layer material thickness of 275 mm, depending on the relative stiffness (or contrast) of the layer materials. A comparison of moduli of granular soils obtained from the SSG with moduli obtained from other tests on the basis of comparable stress levels indicates that the SSG measures moduli in the very small strain amplitude range (i.e. $2{\cdot}7 \times 10^{-4}$ to $4{\cdot}3 \times 10^{-4}$%, which is less than 10^{-3}%). The SSG-induced strain amplitudes are lower than the strain amplitudes induced in the resilient modulus test, but are larger than the strain amplitude of the seismic test.[6]

The measured soil stiffness from the SSG can be used to calculate the modulus of the materials near the surface. For a rigid ring-shaped foot resting on a linear-elastic, homogeneous, and isotropic infinite half-space, the stiffness (K_{SSG}) is related to the modulus of the soil (E_{SSG}):[9]

$$K_{SSG} = \frac{1{\cdot}77\,E_{SSG}\,R}{1-\nu^2} \quad (1)$$

where ν is the Poisson's ratio of the materials, and R is the outside radius of the ring (57·2 mm). Note that K_{SSG} and E_{SSG} are expressed in MN/m and MPa respectively. Because of the very small strain amplitudes induced by the SSG, an elastic response of the soils is assumed, and the use of equation (1) is justified.

2.2. Correlation with other moduli

Back-calculated moduli of base and subgrade soils from the falling weight deflectometer (FWD) test have been used extensively in pavement design, construction and maintenance. Wu *et al.*[10] found that the relationship between the SSG stiffness (K_{SSG}) and the back-calculated modulus from the FWD (E_{FWD}) can be presented in the following form:

$$E_{FWD} = 22{\cdot}96e^{0{\cdot}12K_{SSG}} \qquad R^2 = 0{\cdot}66 \quad (2)$$

Note that K_{SSG} and E_{FWD} are expressed in MN/m and MPa respectively. Wu *et al.*[10] also noted that the difference between these methods can be ascribed to the in-situ variability of the material properties. As E_{FWD} is obtained through inversion based on all seven deflection measurements, which cover a distance of about 2 m, E_{FWD} of pavement layers is therefore a weighted average value over 2 m. By contrast, the SSG measures only the near-surface soil stiffness right underneath its ring foot, with a measurement influence of less than 0·3 m. Chen *et al.*[11] suggested that a general linear relationship between K_{SSG} and E_{FWD} is discernible as the following:

$$E_{FWD} = 37{\cdot}65K_{SSG} - 261{\cdot}96 \qquad R^2 = 0{\cdot}82 \quad (3)$$

Again, K_{SSG} and E_{FWD} are expressed in MN/m and MPa respectively. Wu *et al.*[10] provided the correlation between SSG stiffness and modulus from seismic tests, including dirt-seismic

pavement analyser (D-SPA) and spectral analysis of surface waves (SASW), for soft to medium-stiff subgrades to very stiff bases. They indicated that the modulus obtained from the SSG is about a quarter of that obtained from seismic tests. A linear relationship is obtained between the SSG stiffness (K_{SSG}) and the seismic modulus (E_{SEIS}):

$$E_{SEIS} = 47{\cdot}53K_{SSG} + 79{\cdot}05 \qquad R^2 = 0{\cdot}62 \tag{4}$$

Note that K_{SSG} and E_{SEIS} are expressed in MN/m and MPa respectively. The discrepancy between these two tests is explained by the difference in the stress–strain levels used, as well as by the uncertainty of the effective depth of the SSG, which varies with stiffness, density, and types of materials being tested.[10] Chen *et al.*[11] also conducted a similar study, and indicated that the relationship between K_{SSG} and E_{SEIS} from D-SPA and SASW for soft to medium-stiff subgrades to very stiff bases can be expressed as follows:

$$E_{SEIS} = 55{\cdot}42K_{SSG} - 162{\cdot}94 \qquad R^2 = 0{\cdot}81 \tag{5}$$

Again, the units of K_{SSG} and E_{SEIS} are in MN/m and MPa respectively. The relationship between K_{SSG} and E_{SEIS} is found to be obvious and convincing. The operation of the SSG is very simple and feasible for the purpose of quality control; however, it yields a stiffness value only near the surface. The seismic tests can generate a stiffness–depth profile, but its operation is more complicated.[11]

3. DYNAMIC CONE PENETROMETER (DCP)

3.1. Description

Scala[12] developed the Scala penetrometer for assessing the in-situ CBR of cohesive soils. In the last decade, the Scala penetrometer has evolved into the DCP test for determining in-situ CBR and modulus. The DCP is now being used extensively in South Africa, the United Kingdom, the United States, Australia, and other countries because it is simple, rugged, economical, and able to provide a rapid in-situ index of strength and, more indirectly, the modulus of the subgrade as well as the pavement structure.

The DCP is used for measuring the material resistance to penetration in terms of millimetres per blow while the cone of the device is being driven into the pavement structure or subgrade. The typical DCP consists of an 8 kg hammer that drops over a height of 575 mm, which yields a theoretical driving energy of 45 J or 14·3 J/cm^2, and drives a 60° 20 mm base diameter cone tip vertically into the pavement structure or subgrade (Fig. 1(b)). The steel rod to which the cone is attached has a smaller diameter than the cone (16 mm) to reduce skin friction. The number of blows during operation is recorded with the depth of penetration. The slope of the relationship between number of blows and depth of penetration (in millimetres per blow) at a given linear depth segment is recorded as the DCP penetration index (DPI). In addition to soil profiling (i.e. the thickness and nature of each layer in a given pavement), DCP data are correlated with various pavement design parameters, including CBR, shear strength, modulus, and back-calculated modulus from the FWD.[11,13–17] The DCP has been available longer than the SSG, and has been used as a convenient field tool; however, it is not a direct property test but an index test based on dynamic impact loading.

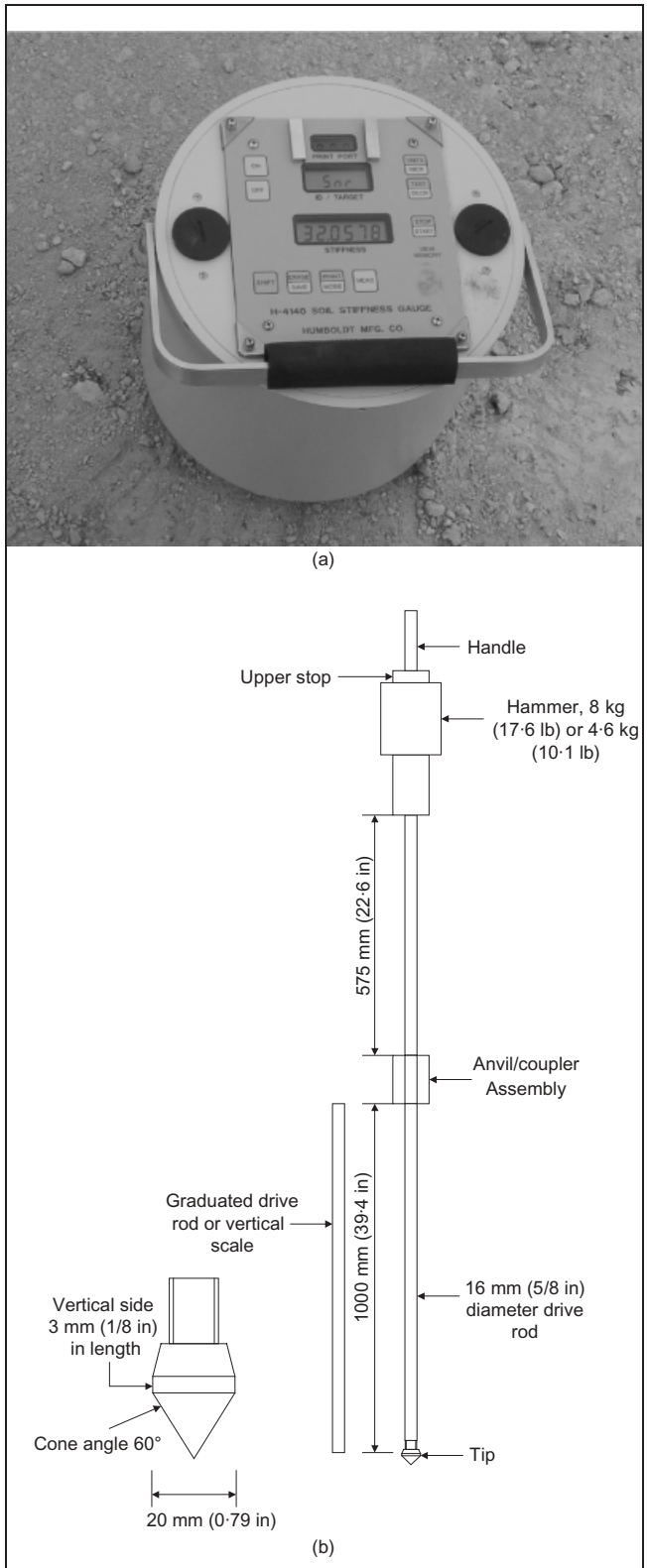

Fig. 1. (a) Humboldt soil stiffness gauge (SSG); (b) dynamic cone penetrometer (DCP)

As DCP testing is basically a measure of penetration resistance, expressed as DCP penetration index (DPI), the analysis of the DCP data must be interpreted, following a standardised procedure, to generate a representative value of penetration per

blow for the material being tested. This representative value can be obtained by averaging the DPI across the entire penetration depth at each test location. Two methods of calculating the representative DPI value for a given penetration depth of interest are considered: (a) arithmetic average and (b) weighted average.[18] The arithmetic average can be obtained as follows:

$$\text{DPI}_{\text{avg}} = \frac{\sum_{i}^{N} (\text{DPI})_i}{N} \quad (6)$$

where N is the total number of DPI recorded in a given penetration depth of interest. The weighted average technique uses the following formula:

$$\text{DPI}_{\text{wt avg}} = \frac{1}{H} \sum_{i}^{N} \left[(\text{DPI})_i \cdot (z)_i \right] \quad (7)$$

where z is the penetration distance per blow set and H is the overall penetration depth of interest. These two methods are graphically presented in Fig. 2 for a lean clay with sand (STH 100 in Table 1). Allbright[19] reported that the weighted average method yielded a narrower standard deviation for the representative DPI value and provided better correlations with other field tests than the arithmetic average method based on available field data. In this study, the weighted average method is employed to calculate the representative DPI value.

The influence of layers below and above the cone tip must also be considered in the analysis of the DCP data. As cone penetration is associated with the development of a failure surface, the penetration resistance is influenced by the presence of a layer if the cone tip is located within a few cone diameters of the interface of two highly contrasting layers. Little effect on penetration resistance is noticed as the cone tip approaches the interface if both layers have similar properties. The extent of the zone of influence depends on the size of the cone, soil type, soil density, stress state, and the contrast in properties of adjacent layers.[20] The weighted average DPI was calculated

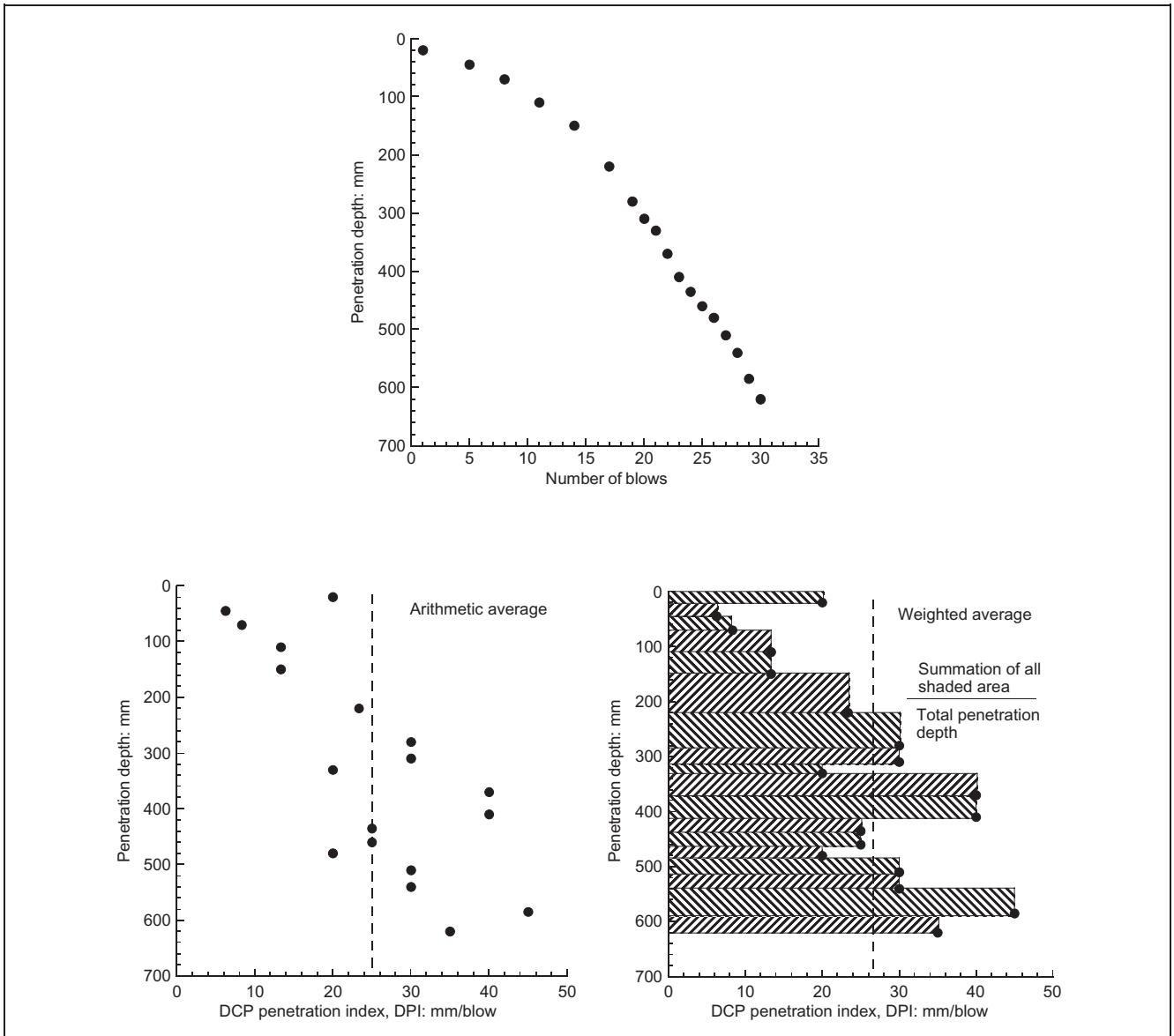

Fig. 2. Two methods for calculating the representative DPI value

Site	Soil name	Specific gravity	Liquid limit	Plasticity index	Classification		W_N: %	W_{OPT}: %	γ_{dmax}: kN/m^3
					USCS	AASHTO			
STH 60 (test section)	Joy silt loam	2·70	39	15	CL-ML	A-6(16)	25·0	19·0	16·5
Scenic Edge development	Plano silt loam	2·71	44	20	CL	A-7-6(20)	27·0	20·0	16·2
Gils Way development	Plano silt loam	2·71	46	20	CL	A-7-6(20)	23·4	19·5	16·3
STH 26	Lean clay with sand	2·64	32	11	CL	A-6(7)	20·7	13·5	19·2
STH 100	Lean clay with sand	2·74	29	14	CL	A-6(9)	14·2	14·4	18·2
STH 44	Silty, clayey sand	2·70	23	7	SM-SC	A-4(0)	9·8	11·7	19·8

Table 1. Properties of natural earthen materials and their classification: fine-grained soils (USCS, unified soil classification system; AASHTO, American Association of State Highway and Transportation Officials)

over various DCP penetration depths, from the surface to 76, 152, 229, 305 and 381 mm, in the analyses to identify the most representative depth in correlating DPI with SSG stiffness. The only exception was the chemically stabilised soils, where the maximum penetration depth was limited by the thickness of the stabilised layer (i.e. 305 mm). As these selected penetration depths over which the DPI was calculated were generally well within a layer, the DPI obtained is considered to have negligible influence from an interface. It has been shown that vertical confinement (i.e. due to rigid pavement structure or upper granular/cohesive layers) and rod friction (i.e. due to a collapse of the granular material on the rod surface during penetration) may affect DPI values.[21] These effects were not an issue in this investigation, because the current study involved only subgrade and subbase evaluation during construction such that the DCP tests were performed directly on the exposed surface of these materials.

3.2. Correlation with California bearing ratio (CBR)

To assess the structural properties of the pavement materials, the DCP penetration index (DPI) values are usually correlated with the California bearing ratio (CBR) of the pavement materials. Extensive research has been conducted to develop an empirical relationship between DPI and CBR for a wide range of pavement and subgrade materials. This include research by Livneh *et al.*,[21] Kleyn,[22] Harison,[23] Livneh,[24] McElvaney and Djatnika,[25] Webster *et al.*,[26] and Livneh and Livneh.[27] Based on their researches, many of the relationships between DPI and CBR can be quantitatively presented in the following form:

$$\log(\mathrm{CBR}) = \alpha + \beta \log(\mathrm{DPI}) \quad (8)$$

where α and β are coefficients ranging from 2·44 to 2·56 and −1·07 to −1·16 respectively, which are valid for a wide range of pavement and subgrade materials. Note also that CBR is in percent and DPI is in millimetres per blow (mm/blow). For a wide range of granular and cohesive materials, the US Army Corps of Engineers use the coefficients α and β of 2·46 and −1·12, which have been also adopted by several agencies and researchers[20,26,28,29] and are in general agreement with the various sources of information. Livneh *et al.*[21] also show that there exists a universal correlation between DPI and CBR for a wide range of pavement and subgrade materials, testing conditions, and technologies. In addition, the relationship between DPI and CBR is independent of water content and dry unit weight, because water content and dry unit weight influence DPI and CBR equally.

4. FIELD TESTING PROGRAMME

4.1. Data collection

A Humboldt SSG manufactured by Humboldt Mfg Co. was used to measure the in-situ stiffness properties of the pavement materials in this study. The SSG stiffness measurements were made in accordance with ASTM D6758.[30] The SSG assesses near-surface stiffness with a maximum measurement depth of approximately 300–380 mm. Sawangsuriya *et al.*[6,8] reported that the depth of measurement significance ranges from 125 to 178 mm, where the higher stress–strain conditions occur within the measurement zone (i.e. 125–300 mm), and this is also beyond a blind zone that exists at less than 125 mm in SSG measurements. These findings were based on granular soils, but similar conditions can also be expected in fine-grained (cohesive) soils.

A DCP manufactured by Kessler Soils Engineering Products, Inc. was used to measure the in-situ strength index properties of the pavement materials in this study. DCP penetration index (DPI), in millimetres per blow, which can be used to estimate the shear strength characteristics of soils, was calculated in accordance with ASTM D6951.[31] The DCP is typically used to assess material properties to a depth of 1 m below the ground surface. The size of the cone tip relative to the average grain size of the material that is penetrated is found to influence the penetration resistance.[20] This is because of the number of grains that come into contact with the face of the cone and the failure surface. Therefore the DCP cannot be used in very coarse-grained materials containing a large percentage of aggregates greater than 50 mm, or in highly stabilised or cemented materials.

4.2. Site description

SSG and DCP measurements were made at 10 highway construction sites around the state of Wisconsin, USA. Test section STH 60 is located approximately 40 km north of the city of Madison, and consists of a 1·4 km segment of the highway. This project consisted of a field demonstration of alternative soft subgrade reinforcement methods. Detailed descriptions of each test section are given in Edil *et al.*[32] The SSG and DCP tests were conducted in each test section.

Scenic Edge development project is a 0·7 km city street constructed as a residential subdivision in Cross Plains by stabilising the soft subgrade in place with fly ash. Both the subgrade soil and the fly-ash-stabilised subgrade layer were tested using the SSG and DCP.

Gils Way development project, which uses a soil–lime mixture, is also located in Cross Plains. The construction section was approximately 400 m long. Because of the time constraint, only the SSG was performed before the liming process—that is, on the untreated subgrade. The SSG and DCP were performed after the liming process—that is, on the lime-stabilised subgrade layer.

Seven highway construction sites that involved the use of only natural earthen materials were from different soil regions of Wisconsin.[18] The SSG and DCP were performed on the exposed subgrade soils that were either compacted (five sites) or had not been re-compacted (two sites).

5. MATERIAL CLASSIFICATION AND PROPERTIES

Samples were collected either along the centreline or near the shoulder of the roadway from 10 highway construction sites to determine the index properties, soil classification, and compaction characteristics. Tables 1 and 2 summarise the natural earthen materials encountered and their properties, together with their classification. Compaction curves corresponding to the standard compaction effort described in ASTM D698[33] were developed, except for breaker run. Note that breaker run is the excavated and crushed rock including cobbles (75–350 mm in diameter) with a soil fraction. It was retrieved from the cuts in parts of the project route. Its soil fraction consisted of approximately 30% gravel, 65% sand, and 5% fines.

The properties of the processed construction materials (i.e. other than the natural earthen materials), along with their classification, are summarised in Tables 3 and 4. These materials are subdivided into two main categories: (a) industrial by-products and (b) chemically stabilised soils. The by-products consisted of bottom ash, foundry slag, and foundry sand. Bottom ash and foundry slag are well-graded coarse-grained sand-like materials, and thus are insensitive to moisture content during compaction. Foundry sand is primarily

Site	Soil name	Specific gravity	D_{10}: mm	D_{60}: mm	C_u	% Fines	Classification		W_{OPT}: %	γ_{dmax}: kN/m^3
							USCS	AASHTO		
USH 12	Clayey sand*	2·69	NA	0·2	NA	34·45	SC	A-2-4(0)	10·0	18·9
STH 131	Poorly graded sand with silt	2·62	0·09	0·35	3·9	6·54	SP-SM	A-3(0)	8·0	18·0
STH 58	Clayey sand†	2·62	NA	0·25	NA	25·50	SC	A-2-4(0)	8·5	19·8
STH 154	Poorly graded sand with silt	2·63	0·07	0·4	5·7	11·46	SP-SM	A-3(0)	9·0	18·7
STH 60 (test section)	Breaker run	NM	0·25	29·0	116	3·12	GW	A-1-a(0)	None	NM

Notes: NM = not measured, NA = not applicable.
* LL = 24, PI = 7.
† LL = 24, PI = 8.

Table 2. Properties of natural earthen materials and their classification: predominantly granular soils (USCS, unified soil classification system; AASHTO, American Association of State Highway and Transportation Officials)

Site	Soil name	Specific gravity	D_{10}: mm	D_{60}: mm	C_u	% Fines	Classification		W_{OPT}: %	γ_{dmax}: kN/m^3
							USCS	AASHTO		
STH 60 (test section)	Bottom ash*	2·65	0·06	1·9	31·7	13·23	SW	A-1-b(0)	None	15·1
	Foundry sand†	2·55	0·0002	0·23	1150	28·92	SC	A-2–7(2)	16·0	16·1
	Foundry slag*	2·29	0·13	2·0	15·4	5·27	SW	A-1-b(0)	None	10·0

* Non-plastic.
† LL = 44, PI = 25.

Table 3. Properties of processed construction materials (industrial by-products) and their classification (USCS, unified soil classification system; AASHTO, American Association of State Highway and Transportation Officials)

Site	Soil name	Chemical stabilised content: %	Stabilised soil (no delay)		Stabilised soil (2 h delay)		Soil component	
			W_{OPT}: %	γ_{dmax}: kN/m^3	W_{OPT}: %	γ_{dmax}: kN/m^3	W_{OPT}: %	γ_{dmax}: kN/m^3
STH 60 (test section)	Fly-ash-stabilised soils	10	20·0	16·6	21·0	16·1	19·0	16·5
Scenic Edge development	Fly-ash-stabilised soils	12	21·0	16·2	21·0	15·6	20·0	16·2
Gils Way development	Lime-stabilised soils	5	NM	NM	NM	NM	19·5	16·3

Note: NM = not measured.

Table 4. Properties of processed construction materials (chemically stabilised soils) and their classification

a mixture of fine sand and sodium bentonite (~10% by weight) that also contains small percentages of other additives. The foundry sand is sensitive to water content when compacted, and exhibits a conventional compaction curve.

Chemical stabilisation involved a mixture of natural soil and either fly ash or lime. The fly-ash-stabilised soil at the STH 60 test section and Scenic Edge development sites was prepared by mixing Class C fly ash with subgrade soil at its natural water content (wetter than the optimum water content). Analysis from a series of mix designs evaluated in the laboratory indicated that the subgrade soil stabilised using a fly ash content of 10% for the STH 60 test section site and 12% for the Scenic Edge development site (on the basis of dry weight) provided sufficient strength and hence was adopted for field construction. The lime-stabilised soil at Gils Way development in Cross Plains was prepared by mixing 5% lime with subgrade soil at its natural water content (wetter than the optimum water content).

6. SSG STIFFNESS AND DCP PENETRATION INDEX (DPI)

Tables 5 and 6 summarise the results of the SSG and DCP measurements made. The mean SSG stiffness and DPI of various materials are also illustrated graphically in Fig. 3. Fly-ash-stabilised soils have the highest mean stiffness, which increases with time of curing. For the lime-stabilised soil, the mean stiffness after liming is nearly twice that of the untreated subgrade. These results clearly indicate that the SSG can be used to monitor increase in stiffness due to stabilisation reactions. In general, the granular earthen materials including breaker run are stiffer than fine-grained earthen materials. Among three types of industrial by-product, foundry sand has the highest stiffness, with bottom ash and foundry slag having nearly half its stiffness.

Dynamic cone penetration is controlled primarily by the strength of a material, and therefore DPI (amount of

Material type	No. of tests*	Mean†	Standard deviation	Coefficient of variation: %	Standard error	Maximum	Minimum
Natural earthen							
Granular	18	7·8	1·88	24	0·44	12·1	5·4
Fine-grained	90	5·6	1·98	35	0·21	11·0	1·6
Industrial by-products							
Bottom ash	4	3·9	0·20	5	0·10	4·1	3·7
Foundry sand	4	7·7	1·07	14	0·54	9·0	6·4
Foundry slag	18	3·1	1·03	33	0·24	4·8	1·5
Fly-ash-stabilised soils							
24 hs	22	12·9	2·85	22	0·67	21·1	7·9
7–8 days	15	15·1	3·75	25	0·97	21·7	7·1
Lime-stabilised soils							
Before liming	15	5·3	1·44	27	0·37	7·0	2·7
After liming	15	9·5	1·59	17	0·41	12·9	6·8
Other							
Breaker run	8	6·7	1·19	18	0·42	8·8	4·5

* Corresponding to total number of test locations in the material category.
† Mean of SSG stiffness for total number of test locations in the material category.

Table 5. Results of soil stiffness gauge (SSG) measurements: stiffness (MN/m)

Material type	No. of tests*	Mean†	Standard deviation	Coefficient of variation: %	Standard error	Maximum	Minimum
Natural earthen							
Granular	18	33·9	20·44	60	4·82	93·3	12·6
Fine-grained	81	44·7	27·89	62	3·10	170·0	12·2
Industrial by-products							
Bottom ash	4	52·7	9·99	19	4·99	63·1	43·8
Foundry sand	3	59·1	16·59	28	9·58	69·8	40·0
Foundry slag	5	49·8	15·92	32	7·12	72·0	32·1
Fly-ash-stabilised soils							
24 h	13	18·4	3·60	20	1·00	26·5	13·4
7–8 days	15	15·2	8·05	53	2·08	39·1	7·1
Lime-stabilised soils							
After liming	15	13·7	1·94	14	0·50	17·3	11·6

Notes: DCP tests were not performed on lime-stabilised soils before liming and breaker run.
DPI was calculated by weighted average over a penetration depth of 152 mm.
* Corresponding to total number of test locations in the material category.
† Mean of weighted average DPI for total number of test locations in the material category.

Table 6. Results of DCP measurements: DCP penetration index (DPI) (mm/blow)

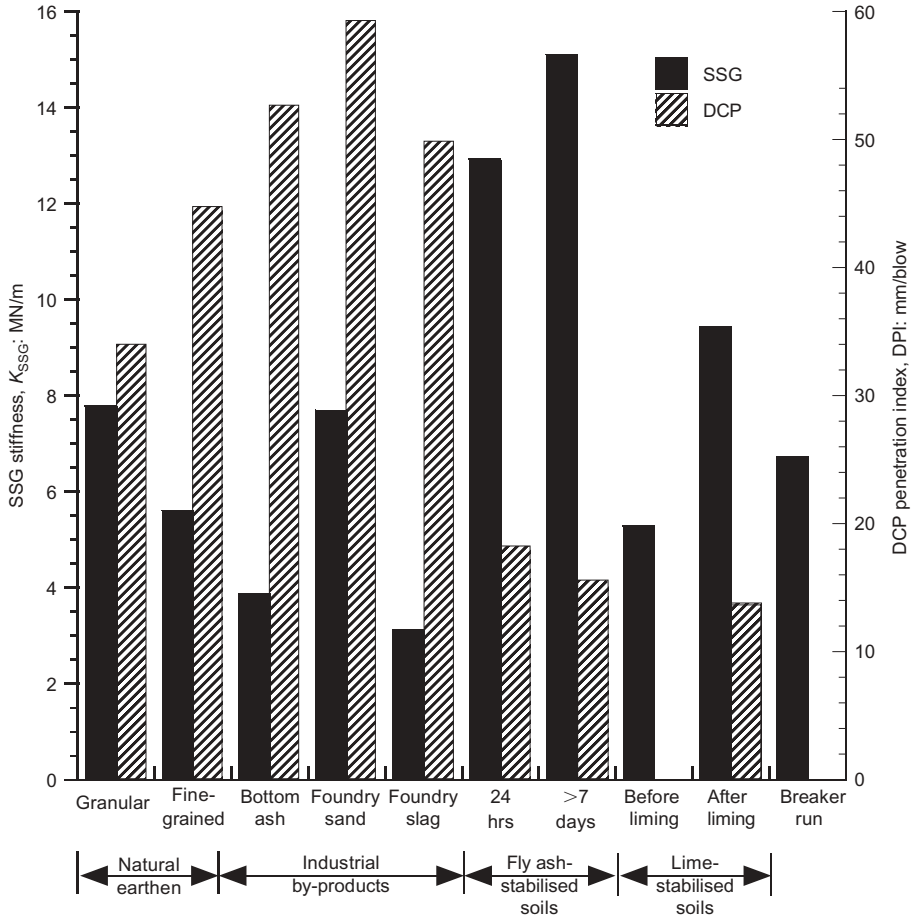

Fig. 3. Mean soil stiffness gauge stiffness and dynamic cone penetrometer penetration index (DPI) values of various materials

penetration per blow) is inversely proportional to shear strength. The patterns exhibited by the DPI, in general, parallel those of the SSG stiffness in Fig. 3 with some exceptions (for example, compare the relative stiffness and strength of industrial by-products and fine-grained soils). The data in Tables 5 and 6 indicate that the standard error associated with DPI is considerably larger than that of the SSG stiffness.

7. CORRELATION BETWEEN SSG STIFFNESS AND DPI VALUES

The correlation of SSG stiffness with DPI is examined based on six material categories:

(*a*) natural earthen materials (both granular and fine-grained soils)
(*b*) granular materials (natural soils, bottom ash and foundry slag)
(*c*) fine-grained (cohesive) soils
(*d*) fly-ash-stabilised soils
(*e*) fine-grained materials including fly-ash-stabilised soils
(*f*) all materials combined, including foundry sand.

Breaker run is not included because the DCP cannot be performed on this material. Foundry sand exhibits both granular and fine-grained material behaviour, so it is only included only in category (*f*). Table 7 summarises the results

Material category	No. of points	Intercept	Slope	R^2	Standard error	*p*-Value
Natural earthen	79	17·9	−7·5	0·60	1·44	0·00
Granular	27	19·3	−8·3	0·55	1·73	0·00
Fine-grained soils	52	17·1	−7·1	0·64	1·28	0·00
Fly-ash-stabilised soils	37	24·8	−10·0	0·40	2·05	0·00
Fine-grained + fly-ash-stabilised soils	89	26·7	−12·7	0·75	2·16	0·00
All combined (includes foundry sand)	119	25·6	−12·0	0·72	2·15	0·00

Note: DPI was calculated by weighted average over a penetration depth of 152 mm from the surface.

Table 7. Parameters of linear regression analysis for relationship of SSG stiffness (MN/m) to log DPI (mm/blow)

of the linear regression analyses between SSG stiffness and log DPI in these material categories. Only those tests that were conducted at the same location are included in the analysis. For all material categories in Table 7, the best correlations (i.e. highest R^2) were obtained when DPI was averaged over a DCP penetration depth of 152 mm after examining correlations of average DPI calculated over varying DCP penetration depths.[18] It is also noted that, for natural subgrade soils, a better correlation was obtained after they were compacted,[18] probably because of the more uniform conditions, which result in a reduction of the dispersion of the data. Fig. 4 illustrates the correlation between stiffness and DPI for all materials combined. The SSG stiffness is related to DPI in a simple linear semi-logarithmic relationship. The dispersion of the data is explainable to a degree by the fact that, although stiffness and strength are related in a general sense, there is not always a one-to-one relationship, as demonstrated in Fig. 3. Nonetheless, the SSG stiffness and DPI correlate well, with an R^2 of 0·72.

8. CORRELATION BETWEEN MODULUS AND CBR (ALSO DPI)

8.1. Previous research

Empirical correlations between modulus (E) and CBR (also DPI) have been proposed by a number of researchers. A well-known UK Transportation Research Laboratory (TRL) equation developed between modulus (E) and CBR of the subgrade soil has been given by Powell *et al.*[3] This equation has been established primarily from the comprehensive data relating modulus measured by wave propagation to *in situ* CBR tests on both remoulded and undisturbed subgrade soils.[34] After taking into account the effects of the very low strain levels generated in the wave propagation technique, and other information obtained from repeated load triaxial tests conducted at realistic stress levels and *in situ* measurements of transient stress and strain in experimental pavements, the modulus from the seismic test was adjusted, and the corresponding equation is expressed as follows:[3]

$$E_{\text{SEIS-MOD}} = 17{\cdot}6 \times \text{CBR}^{0{\cdot}64} \quad (9)$$

Note that, for the sake of clarity, the modulus used in equation (9) is denoted as the modulus from the seismic test after adjustment to realistic stress and strain levels for the pavement ($E_{\text{SEIS-MOD}}$). $E_{\text{SEIS-MOD}}$ and CBR units are in MPa and percent respectively.

Another well-known relationship, which is widely used in North America, is the one proposed by Heukelom and Foster.[35] It has been adopted by the American Association of State Highway and Transportation Officials (AASHTO) in the *Guide for Design of Pavement Structures*:[36]

$$E_{\text{RM}} = 10 \times \text{CBR} \quad (10)$$

where E_{RM} is the modulus from the resilient modulus test, in MPa.

In addition to these two well-known relationships, Chen *et al.*[37] suggested the following relationship between back-calculated moduli from the FWD (E_{FWD}) and DPI:

$$E_{\text{FWD}} = 338 \times \text{DPI}^{-0{\cdot}39} \quad (11)$$

where E_{FWD} and DPI are in units of MPa and millimetres per blow (mm/blow) respectively.

Konrad and Lachance[20] presented a relationship between DPI using a 51 mm diameter cone and modulus of unbound aggregates, gravelly, and sandy soils back-calculated from plate load tests (E_{PLT}) by the following equation:

$$\log(E_{\text{PLT}}) = -0{\cdot}884 \log(\text{DPI}) + 2{\cdot}906 \quad (12)$$

where DPI is the DCP penetration index in millimetres per blow (mm/blow) using a 51 mm diameter cone and a 63·5 kg hammer dropping 760 mm, and E_{PLT} is expressed in MPa.

Livneh and Goldberg[38] carried out comparative German light drop weight (LDW) and DCP tests. The relationship between the modulus measured by the LDW (E_{LDW}) and the *in situ* CBR values obtained from the DCP is expressed as follows for clayey and sandy soils respectively:

$$E_{\text{LDW}} = 600 \times \ln \frac{300}{300 - 6{\cdot}019 \times \text{CBR}^{(1/1{\cdot}41)}} \quad (13)$$

$$E_{\text{LDW}} = 600 \times \ln \frac{300}{300 - 4{\cdot}035 \times \text{CBR}^{(1/1{\cdot}41)}} \quad (14)$$

where E_{LDW} and CBR are in units of MPa and percent respectively.

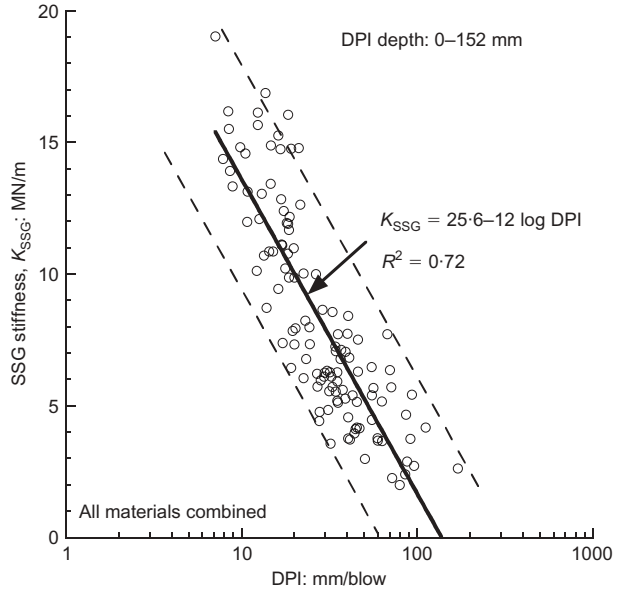

Fig. 4. Relationship between SSG stiffness and DPI for all materials combined

8.2. Development of empirical correlations

After a simple linear semi-logarithmic relationship between SSG stiffness (K_{SSG}) and DPI values was determined (i.e. $K_{SSG} = 25{\cdot}6 - 12 \log \mathrm{DPI}$) based on direct regression from the actual measured data for all materials combined (Fig. 4), such a correlation can be further developed to become a more meaningful and useful equation, which can be used in the design of pavements. To accomplish this, the measured SSG stiffness is converted to the SSG modulus (E_{SSG}) of the pavement materials using equation (1). Values for Poisson's ratio (ν) of the granular soils including foundry slag and bottom ash were assumed to be 0·40. For fly-ash-stabilised soils and fine-grained soils including foundry sand, ν values of 0·25 and 0·35 were used. These values were selected according to their typical ranges suggested by Huang.[39] Similarly, the weighted average DPI value obtained from the DCP can be converted to the CBR of the pavement materials using the well-established correlation given in equation (8) with the coefficients α and β of 2·46 and $-1{\cdot}12$ respectively. Fig. 5 illustrates a plot of calculated SSG modulus (E_{SSG}) against CBR from the DCP. The regression equation obtained is expressed as follows:

$$E_{SSG} = 18{\cdot}77 \times \mathrm{CBR}^{0{\cdot}63} \qquad R^2 = 0{\cdot}74 \tag{15}$$

where the units of E_{SSG} and CBR are MPa and percent respectively. It can be seen that a unique relationship exists between E_{SSG} and CBR, regardless of soil type and site, although the coefficient of correlation of equation (15) is inherently dependent on the coefficient of correlation of equation (8). The results of SSG tests and DCP tests are expected to be affected by the same factors (i.e. relating the two test results directly excludes the influence of water content, dry density, and other basic indices). Furthermore, such a relationship is not affected by change in pavement condition, and is also applicable to both the as-compacted and post-construction states. This equation yields almost identical values to those obtained from the equation given by Powell *et al.*[3]—that is, equation (9). Fig. 6 illustrates the comparison between moduli from the SSG (E_{SSG}) and those from the DCP (E_{DCP}) using the regression equations given in equations (8) and (9). Remarkably good agreement is obtained with an independent, widely used approach.

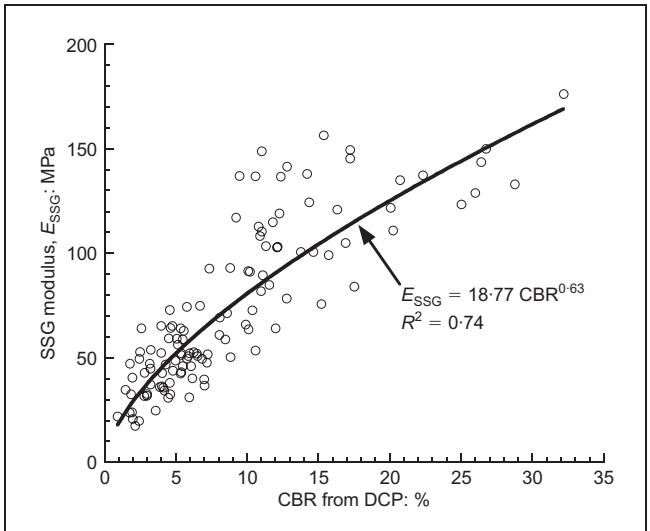

Fig. 5. Correlation between modulus from the SSG and CBR from the DCP

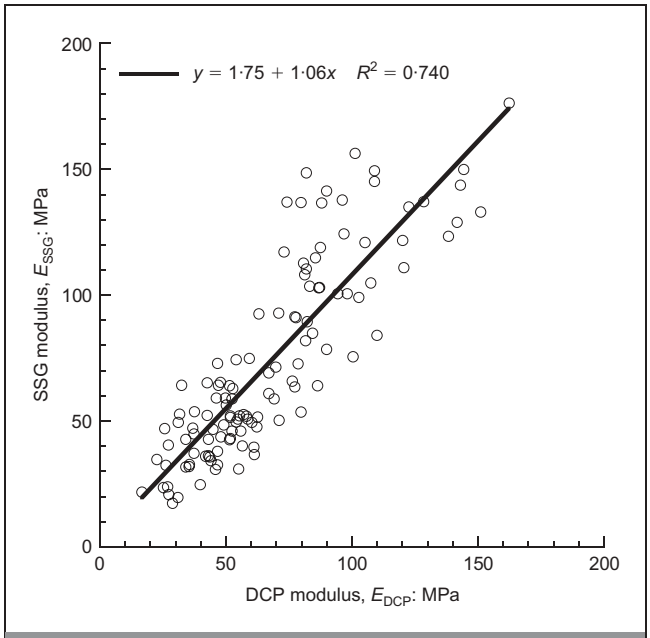

Fig. 6. Comparison between moduli from the SSG and those from the DCP

A regression equation obtained in this study is also compared with that obtained from different in-situ tests including the FWD, LWD and plate load tests, as shown in Fig. 7. The equations obtained for the FWD, LWD and plate load test are given by Chen *et al.*,[37] Livneh and Goldberg,[38] and Konrad and Lachance[20] respectively. Note also that the parameter DPI in equations (11) and (12) can be converted to CBR using equation (8) with the coefficients α and β of 2·46 and $-1{\cdot}12$ respectively. The comparison results suggest that the regression equation obtained in this study is best correlated to the equation given by Powell *et al.* (i.e. equation (9)), established between modulus and CBR.[3] Within CBR values ranging from 0% to 20%, the FWD and LWD (on sand) tests, respectively, provide the highest and lowest E for a given CBR. The

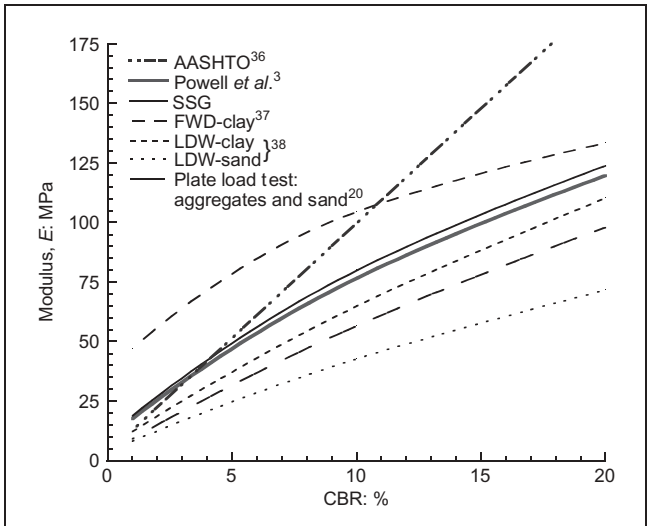

Fig. 7. E–CBR relationship of different methods

relationship from the plate load test is in between the curve of equation (9) and the LDW test (on sand). The suggested equation by AASHTO[36] gives the highest modulus when the CBRs are greater than 10%. Large deviation from the other modulus tests is observed at relatively high CBRs as well. Using Fig. 7, the modulus can be estimated for any pavement condition if CBR is obtained for the corresponding condition. It is perhaps not surprising that the modulus given in equation (9) by Powell *et al.* and the SSG modulus given in equation (15) as developed in this study as a function of CBR agree well. The reason might be that both moduli were adjusted to realistic strain amplitude and stress levels from those corresponding to the wave propagation technique. According to Powell *et al.*, their moduli were adjusted to strain amplitude and stress level in pavements from those corresponding to the wave propagation technique. In the case of the SSG, it was shown by Sawangsuriya *et al.*[6] that the SSG modulus corresponds to strain amplitudes larger than the strain amplitudes of the wave propagation technique, even though the SSG induces strain amplitudes comparable to that of the wave propagation technique. In fact, the stress and strain levels induced by the SSG are 2 kPa and less than 10^{-3}% respectively. It has also been shown that a somewhat reduced modulus is reported by the internal computation of the SSG device.[6]

8.3. Model validation

To verify the power model given in equation (15), field measurement data from another two test sites were plotted onto the developed power model and Powell's equation, as shown in Fig. 8. The test sites were a section of State Trunk Highway (STH) 32 located in Port Washington, and a section of STH 12 located between Cambridge and Fort Atkinson, both in Wisconsin, USA. The SSG and DCP data from these sites were obtained recently, and were not included in the development of equation (15). The predominant subgrade soil of STH 32 is clayey sand classified as SC and A-4(0) according to the Unified Soil Classification System (USCS) and the AASHTO classification system respectively. The predominant subgrade soil of STH 12 comprises lean clay with sand (CL or A-6(15)) and clayey sand with gravel (SC or A-2–6(0)). Results show that both the developed model (equation (15)) and Powell's equation fit reasonably well to the data set from STH 12 and STH 32, and thus equation (15) appears to be useful for estimating the subgrade modulus. Additionally, the equation suggested by AASHTO[36] overestimates the subgrade modulus for soils with relatively high CBRs.

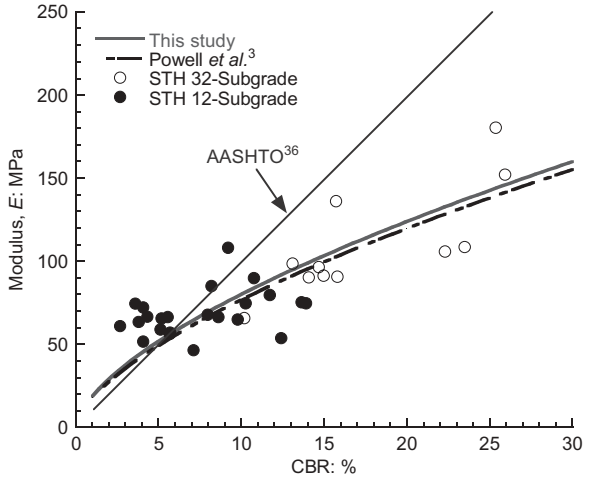

Fig. 8. Comparison of predicted subgrade moduli at STH 32, Wisconsin

9. CORRELATION BETWEEN MODULUS TEST AND UNCONFINED COMPRESSION TEST

In addition to the correlation with CBR from the DCP, the modulus from the SSG can be correlated with the strength from the conventional unconfined compression test. Lee *et al.*[5] suggested an empirical correlation between the modulus from the resilient modulus test (AASHTO T274-82)[40] (E_{RM}) and the stress causing 1% axial strain ($S_{u1\cdot0\%}$) in the conventional unconfined compressive test (ASTM D2166)[41] for the cohesive soils sampled from five in-service subgrades. The relationship is as follows:

$$E_{RM} = 10\,748{\cdot}4 + 5744{\cdot}9S_{u1\cdot0\%} - 48S_{u1\cdot0\%}^2 \quad (16)$$

where the units of E_{RM} and $S_{u1\cdot0\%}$ are both kPa. Note that the E_{RM} values used to develop equation (16) are at an axial deviator stress ($\sigma_1 - \sigma_3$) of 41·4 kPa and a confining stress (σ_3) of 20·7 kPa. $S_{u1\cdot0\%}$ was found to have the best correlation with E_{RM}, compared with other variables (i.e. in-service water content and dry density), and was chosen as a predictor variable instead of the unconfined compressive strength because its strain level is comparable to those of the resilient modulus test, and the stresses at smaller axial strains may have a larger error due to incorrect readings or imperfect contact between the specimen and top cap.[5]

In this study, the moduli from the SSG (E_{SSG}) conducted on subgrade soils at STH 60 (test section) are correlated with the $S_{u1\cdot0\%}$ values from the conventional unconfined compression test. Unconfined compression tests were conducted following ASTM D2166[41] on undisturbed specimens (50 mm in diameter and 100 mm high) trimmed from the tube samples. The test was performed using a strain rate of 2%/min, and the stress at about 1% axial strain was reported. A regression analysis was conducted to obtain a relationship between E_{SSG} and $S_{u1\cdot0\%}$, and the coefficient of determination (R^2) for this relationship is 0·64. A plot of E against $S_{u1\cdot0\%}$ was made, as shown in Fig. 9, in order to compare the correlation results obtained with equation (16). At a similar $S_{u1\cdot0\%}$, the E_{SSG} value is higher than E_{RM} obtained from equation (16), and, as $S_{u1\cdot0\%}$ increases, the difference between E_{SSG} and E_{RM} also increases. This difference may be attributed to the fact that the E_{RM} values used in equation (16) are at higher stress and hence higher corresponding strain levels, whereas the E_{SSG} are measured at much lower stress–strain levels.[6]

10. SUMMARY AND CONCLUSIONS

Soil stiffness gauge and DCP survey data of natural earthen materials, industrial by-products, chemically stabilised soils, and other materials from ten construction sites around the state of Wisconsin are presented, along with their correlation with each other. The data display considerable dispersion, characteristic of the conditions and sampling sizes typical during construction. SSG provides in-situ, near-surface soil stiffness averaged over a limited zone, whereas DCP provides

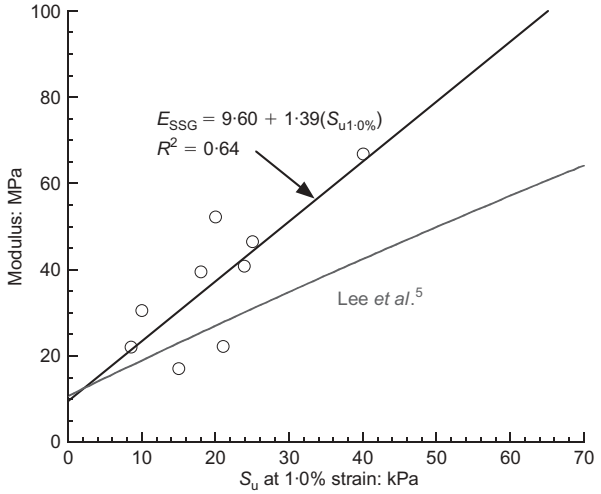

Fig. 9. Relationship between E and $S_{u1·0\%}$ for undisturbed subgrade soils at STH 60 (test section), Wisconsin

individual points of an index of in-situ shear strength expressed as DCP penetration index (DPI) as a function of depth. Therefore each relates to a fundamentally different material property, and is presented in a spatially different manner. To deal with the latter issue, a weighted average of DPI over the depth of measurement is employed to obtain a representative strength index of the material. This approach provided better correlations than the arithmetic average. It is also noted that the standard error associated with DPI is considerably larger than that of the SSG stiffness, which reflects the nature of the two tests.

A simple linear semi-logarithmic relationship is observed between SSG stiffness and DPI. DPI weighted average over a DCP penetration depth of 152 mm yields the highest coefficient of determination, and also yields a statistically significant relationship between the SSG stiffness and DPI for most materials. This depth is consistent with the significant depth of measurement for the SSG, as shown in previous studies. The relationship is indicative of the fact that, although there is not always a one-to-one relationship, stiffness and strength are related in a general sense.

The results of the regression analysis show that there is a significant correlation between the CBR obtained from the DCP and the modulus obtained from the SSG. A power model developed between these two properties is found to be in good agreement with the well-known equation given by Powell *et al.*[3] An equation suggested by AASHTO[36] tends to overestimate the pavement modulus for relatively high CBRs. The modulus from the SSG is also correlated well with the axial stress at 1% strain in the conventional unconfined compression test.

The modulus and CBR are affected in a similar manner by changes of pavement condition, and the relationship between modulus and CBR may be similar for a given soil under any condition if the soil was initially compacted by the same method. Therefore the modulus for the as-compacted or the post-construction states may be estimated from Fig. 7, if CBR is measured or estimated from DCP on the subbase and subgrade materials being subjected to the same conditions.

The study indicates that either or both devices show good potential for future use in pavement and subgrade property evaluation during the construction phase. The in-situ stiffness and strength properties of various materials can be rapidly and directly monitored in companion with the conventional compaction control tests (i.e. nuclear density or laboratory moisture content samples) during earthwork construction. Stiffness and strength are material properties that are needed in different phases of highway design, both for long-term pavement performance and for working platform support and stability during construction. For post-construction conditions, the modulus can be monitored using DCP and the correlations provided, as direct access for SSG is not convenient. The experience both with recycled and reclaimed materials and with chemically stabilised soils is limited compared with natural earthen materials in terms of moisture–density relationships and the related mechanical behaviour. Direct monitoring of stiffness and strength of these new materials using these two devices also appears to be as effective as in natural earthen materials.

11. ACKNOWLEDGEMENTS

This research was funded by the Wisconsin Department of Transportation (WisDOT), USA. The contents of this paper are those of the authors, and do not reflect the opinions or policies of WisDOT. The senior author gratefully acknowledges financial support through a scholarship from the Royal Thai Government. The authors acknowledge Robert Allbright, David Staab, Mark Fredrickson, and Bert Trzebiatowski for their assistances with the laboratory and field tests, and Drs Craig Benson and Peter Bosscher for their suggestions. Thanks are due to Dr Aykut Senol for providing the unconfined compression test data. Finally, the authors also express their sincere gratitude to Robert Arndorfer and other WisDOT personnel for their cooperation in arranging access to the sites.

REFERENCES

1. PINARD M. I. Innovative compaction techniques for improving the bearing capacity of roads and airfields. *Proceedings of the 5th International Conference on the Bearing Capacity of Roads and Airfields, Trondheim*, 1998, 3, 1471–1480.
2. FLEMING P. R. Recycled bituminous planings as unbound granular materials for road foundations in the UK. *Proceedings of the 5th International Conference on the Bearing Capacity of Roads and Airfields, Trondheim*, 1998, 3, 1581–1590.
3. POWELL W. D., POTTER J. F., MAYHEW H. C. and NUNN M. E. *The Structural Design of Bituminous Roads*. Transportation and Road Research Laboratory, Crowthorne, 1984, TRRL Laboratory Report 1132.
4. BROWN S. F. The relationship between California bearing ratio and elastic stiffness for compacted clays. *Ground Engineering*, 1990, 23, No. 8, 27–31.
5. LEE W., BOHRA N. C., ALTSCHAEFFL A. G. and WHITE T. D. Resilient modulus of cohesive soils and the effect of freeze-thaw. *Canadian Geotechnical Journal*, 1995, 32, No. 4, 559–568.
6. SAWANGSURIYA A., EDIL T. B. and BOSSCHER P. J. Relationship between soil stiffness gauge modulus and other test moduli for granular soils. *Transportation*

Research Record 1849, TRB, National Research Council, Washington, DC, 2003, pp. 3–10.
7. LIVNEH M. Validation of correlations between a number of penetration tests and in situ California bearing ratio tests. *Transportation Research Record 1219*, TRB, National Research Council, Washington, DC, 1989, pp. 56–67.
8. SAWANGSURIYA A., BOSSCHER P. J. and EDIL T. B. Laboratory evaluation of the soil stiffness gauge. *Transportation Research Record 1808*, TRB, National Research Council, Washington, DC, 2002, pp. 30–37.
9. EGOROV K. E. Calculation of bed for foundation with ring footing. *Proceedings of the 6th International Conference on Soil Mechanics and Foundation Engineering*, Montreal, 1965, **2**, 41–45.
10. WU W., ARELLANO M., CHEN D.-H., BILYEU J. and HE R. *Using a Stiffness Gauge as an Alternative Quality Control Device in Pavement Construction*. Texas Department of Transportation, Austin, TX, 1998.
11. CHEN D.-H., WU W., HE R., BILYEU J. and ARRELANO M. Evaluation of in situ resilient modulus testing techniques. In *Recent Advances in the Characterization of Transportation Geo-Materials*. GSP No. 86, ASCE, 1999, pp. 1–11.
12. SCALA A. J. Simple methods of flexible pavement design using cone penetrometers. *New Zealand Engineering*, 1956, **11**, No. 2, 34–44.
13. KLEYN E. G., MAREE J. H. and SAVAGE P. F. Application of a portable pavement dynamic cone penetrometer to determine in situ bearing properties of road pavement layers and subgrades in South Africa. *Proceedings of the 2nd European Symposium on Penetration Testing*, Amsterdam, The Netherlands, 1982, 277–282.
14. CHUA K. M. Determination of CBR and elastic modulus of soils using a portable pavement dynamic cone penetrometer. *Proceedings of the 1st International Symposium on Penetration*, Orlando, 1988, 407–414.
15. NEWCOMB D. E., CHADBOURN B. A., VAN DEUSEN D. A. and BURNHAM T. R. *Initial Characterization of Subgrade Soils and Granular Base Materials at the Minnesota Road Research Project*. Minnesota Department of Transportation, St Paul, MN, 1996, MN/RC 96-19.
16. SYED I. and SCULLION T. In-place engineering properties of recycled and stabilized pavement layers. *Proceedings of the 5th International Conference on the Bearing Capacity of Roads and Airfields*, Trondheim, 1998, **3**, 1619–1630.
17. SAARENKETO T., SCULLION T. and KOLISOJA P. Moisture susceptibility and electrical properties of base course aggregates. *Proceedings of the 5th International Conference on the Bearing Capacity of Roads and Airfields*, Trondheim, 1998, **3**, 1401–1410.
18. EDIL T. B. and SAWANGSURIYA A. *Investigation of the DCP and SSG as Alternative Methods to Determine Subgrade Stability*. Wisconsin Department of Transportation, Madison, WI, 2004, Report No. 0092-45-18.
19. ALLBRIGHT R. L. *Evaluation of the Dynamic Cone Penetrometer and its Correlations with Other Field Instruments*. MS thesis, Department of Civil and Environmental Engineering, University of Wisconsin-Madison, 2002.
20. KONRAD J.-M. and LACHANCE D. Use of in situ penetration tests in pavement evaluation. *Canadian Geotechnical Journal*, 2001, **38**, No. 5, 924–935.
21. LIVNEH M., ISHAO I. and LIVNEH N. A. Effect of vertical confinement on dynamic cone penetrometer strength values in pavement and subgrade evaluations. *Transportation Research Record 1473*, Transportation Research Board, National Research Council, Washington, DC, 1995, pp. 1–8.
22. KLEYN, E. G. *The Use of the Dynamic Cone Penetrometer (DCP)*. Transvaal Roads Department, South Africa, 1975, Report No. 2/74.
23. HARISON J. A. Correlation between California bearing ratio and dynamic cone penetrometer strength measurement of soils. *Proceedings of the Institution of Civil Engineers, Part 2*, 1987, **83**, Technical Note No. 463, 833–844.
24. LIVNEH M. Validation of correlations between a number of penetration tests and in situ California bearing ratio tests. *Transportation Research Record 1219*, Transportation Research Board, National Research Council, Washington, DC, 1987, pp. 56–67.
25. MCELVANEY J. and DJATNIKA B. I. Strength evaluation of lime-stabilised pavement foundations using the dynamic cone penetrometer. *Australian Road Research*, 1991, **21**, No. 1, 40–52.
26. WEBSTER S. L., GRAU R. H. and WILLIAMS T. P. *Description and Application of Dual Mass Dynamic Cone Penetrometer*. US Army Engineers Waterways Experimental Station, Vicksburg, MS, 1992, Instruction Report GL-92-3.
27. LIVNEH M. and LIVNEH N. A. Subgrade strength evaluation with the extended dynamic cone penetrometer. *Proceedings of the 7th International Association of Engineering Geology Congress*, Lisbon, Portugal, 1994, Part 1, p. 219.
28. SIEKMEIER J. A., YOUNG D. and BEBERG D. Comparison of the dynamic cone penetrometer with other tests during subgrade and granular base characterization in Minnesota. In *Nondestructive Testing of Pavements and Back Calculation of Moduli*. American Society for Testing and Materials, West Conshohocken, PA, 1999, STP 1375, 175–188.
29. CHEN D.-H., WANG J.-N. and BILYEU J. Application of the dynamic cone penetrometer in evaluation of base and subgrade layers. *Transportation Research Record 1764*, Transportation Research Board, National Research Council, Washington, DC, 2001, pp. 1–10.
30. ASTM. *Standard Test Method for Measuring Stiffness and Apparent Modulus of Soil and Soil-Aggregate In-Place by an Electro-Mechanical Method*. American Society for Testing and Materials, West Conshohocken, PA, 2002, D6758.
31. ASTM. *Standard Test Method for Use of the Dynamic Cone Penetrometer in Shallow Pavement Applications*. American Society for Testing and Materials, West Conshohocken, PA, 2003, D6951.
32. EDIL T. B., BENSON C. H., BIN-SHAFIQUE S., TANYU B. F., KIM W.-H. and SENOL A. Field evaluation of construction alternatives for roadway over soft subgrade. *Transportation Research Record 1786*, Transportation Research Board, National Research Council, Washington, DC, 2002, pp. 36–48.
33. ASTM. *Standard Test Methods for Laboratory Compaction Characteristics of Soil Using Standard Effort* (12,400 ft-lbf/ft^3 (600 kN-m/m^3)). American Society for Testing and Materials, West Conshohocken, PA, 2000, D698.
34. JONES R. In situ measurements of the dynamic properties of

soil by vibration methods. *Géotechnique*, 1958, **8**, No. 1, 1–21.
35. HEUKELOM W. and FOSTER C. R. Dynamic testing of pavements. *Journal of the Soil Mechanics and Foundations Division, ASCE*, 1960, **86**, No. SM1, 1–28.
36. AASHTO. *Guide for Design of Pavement Structures*. American Association of State Highway and Transportation Officials, Washington, DC, 1993.
37. CHEN J., HOSSAIN M., and LATORELLA T. M. Use of falling weight deflectometer and dynamic cone penetrometer in pavement evaluation. *Transportation Research Record 1655*, Transportation Research Board, National Research Council, Washington, DC, 1999, pp. 145–151.
38. LIVNEH M. and GOLDBERG Y. Quality assessment during road formation and foundation construction: use of falling-weight deflectometer and light drop weight. *Transportation Research Record 1755*, Transportation Research Board, National Research Council, Washington, DC, 2001, pp. 69–77.
39. HUANG Y. H. *Pavement Analysis and Design*. Prentice Hall, Englewood Cliffs, NJ, 1993.
40. AASHTO. *Standard Method of Test for Resilient Modulus of Subgrade Soils*. American Association of State Highway and Transportation Officials, Washington, DC, 1986, T 274-82.
41. ASTM. *Standard Test Method for Unconfined Compressive Strength of Cohesive Soil*. American Society for Testing and Materials, West Conshohocken, PA, 2000, D2166.